MAUSAM, **77**, 1 (January 2026), 1-14

MAUSAM

DOI: https://doi.org/10.54302/mh3rsm31
Homepage: https://mausamjournal.imd.gov.in/index.php/MAUSAM

UDC No. 551.583:551.551.577(540)

Climate change trend assessment of precipitation for historic and future period in Palar river basin, India

NANDINI KRISHNAN[1] and SURIYA SARAVANAN[2*]

[1] *Research Scholar, Department of Civil Engineering, Anna University, Chennai, India*

[2] *Associate Professor, Department of Civil Engineering, Mepco Schlenk Engineering College, Sivakasi, India*

(*Received 6 January 2023, Accepted 13 June 2025*)

***Corresponding author's email: suriya.svu@gmail.com**

सार – अध्ययन का अभिद्रश्यक भारत में पलार नदी बेसिन में ऐतिहासिक और भविष्य की वर्षा का विश्लेषण करना है। भारत मौसम विज्ञान विभाग का 1901 - 2020 का ग्रिडयुक्त वर्षाका डेटा, और 2025 - 2099 के लिए सबसे उपयुक्त NEX-GDD डेटा का सालाना और मौसमी समयमानपर विश्लेषण किया गया। "टेलर डायग्राम" और "एफिशिएंसी क्राइटेरिया" का उपयोग करके परफॉर्मेंस क्राइटेरिया के विश्लेषण से पता चला कि MIROC ESM GCM सबसे उपयुक्तजलवायु मॉडल है जो अध्ययनक्षेत्र की जलवायु संबंधी स्तिथिको दर्शाता है। मैन-केंडल परीक्षण से ऐतिहासिक और मध्यम उत्सर्जनपरिदृश्य के लिए सालाना समयमानमें काफी बढ़तीप्रवृत्ति का पता चलता है। ऐतिहासिक वर्षा और समयपरिवर्तनशीलता के साथ बदलाव भविष्य के जलवायुपरिदृश्य की तुलना में कम स्पष्ट हैं। 120 वर्षों (1901-2020) में वर्षा की भिन्नताका औसत प्रमाण(प्रत्येक) ग्रिड बिंदु पर 0.148 mm/वर्ष कम हो गई है। MIROC ESM GCM से भविष्य के जलवायुप्रक्षेपण में दोनों उत्सर्जनपरिदृश्य में वर्षा का दर बड़ाहुआदिखा। RCP 4.5 परिदृश्य में, सालाना वर्षा में बढ़तीप्रवृत्ति दिख रही है और 21वीं सदी के आखिर तक, सभी ग्रिड बिंदु पर औसत वर्षा में 75 mm की बढ़ोतरी देखी जाएगी। RCP 8.5 परिदृश्य में, वर्षा के प्रक्षेपण में कोई प्रवृत्तिप्रतिरूप नहीं दिखता है, लेकिन यह 0.25 mm/वर्ष बढ़ जाता है। 21वीं सदी के पहले दशक में, असल वर्षा मध्यम उत्सर्जनपरिदृश्य जैसी है, और दूसरे दशक में, प्रतिरूप उच्चउत्सर्जनपरिदृश्य जैसा है। आधारभूत अवधि (2000-2020) की तुलना में बेसिन में मध्यम उत्सर्जनपरिदृश्य में 12% और हाई उत्सर्जनपरिदृश्य में 7% वर्षा बढ़ेगी। अध्ययनके नतीजों से समेकितजल संसाधन प्रबंधनमें, चरम घटनाओं को कम करने में और सतत विकासमें फायदा होगा।

ABSTRACT. The objective of the study is to analyse historical and future precipitation in the Palar River Basin, India. India Meteorological Department gridded precipitation data for 1901 – 2020, and the best-fitted NEX-GDDP data for 2025 – 2099 are analysed for annual and seasonal timescales. The analysis of the performance criteria using the Taylor diagram and the efficiency criteria revealed that MIROC ESM GCM is the most appropriate climate model that represents the climatic conditions of the study area. The Mann–Kendall's test reveals a significantly increasing trend in the annual time scale for historical and moderate emission scenarios. Historical precipitation and temporal variability are less pronounced compared to future climate scenarios. The average magnitude of rainfall variation over 120 years (1901-2020) has reduced by 0.148 mm/year at each grid point. The future climate projection from MIROC ESM GCM showed an increased precipitation rate in both emission scenarios. In the RCP 4.5 scenario, the annual rainfall shows an increasing trend and at the end of 21st century, 75 mm increase in average rainfall will be observed in all the grid points. In RCP 8.5 scenario, the precipitation projection shows no trend pattern, but it increases by 0.25 mm/year. In the first decade of the 21st century, actual precipitation resembles the moderate emission scenario, and in the second decade, the pattern resembles the high emission scenario. Relative to the baseline period (2000-2020) the basin would receive a precipitation increase of 12% in the moderate emission scenario and 7% in the high emission scenario. The study results would benefit integrated water resource management, mitigation of extreme events, and sustainable development.

Key words – Rainfall variability, Mann-Kendall test, Sen slope, Taylors diagram, GCM.

1. Introduction

Hydrological system studies are seeking more attention due to the circulation of the bio-geocycle in the system (Fowler and Hennessy, 1995). Excessive precipitation and increased temperature in the basin affect extreme climate events such as floods and droughts (Jayanthi and Keesara, 2020). India's climate change is

having a significant impact on water resources, agriculture, forestry, and health sectors (Majra and Gur, 2009). Under climate change, developing countries like India are more vulnerable to urban floods and droughts that cause significant economic losses (Jena and Azad, 2021). Due to the increase in extreme precipitation events, the impacts of climate change due to flooding are severely affecting the Indian river basins in low-lying flood plains regions (Yadav *et al*., 2014). Due to improper land use management practices, groundwater recharge was reduced, affecting agricultural productivity. Several studies on climate variables and their future projections help to develop the adaptation strategies based on the impact (Ramachandran *et al*., 2019; Panda, 2019). The first step in determining the possible causes is to perform a trend analysis. Precipitation and temperature changes are the prominent meteorological drivers that can explain the occurrence of an increasing or decreasing trend in a hydrologic time series. This key driving parameter in the hydrological cycle affects regional and global climate change. Several statistical techniques have been used to detect significant trends in climate variables that include parametric and non-parametric tests.

Many researchers have investigated the trends of precipitation and temperature all over the world. Studies have shown more robust rising temperature trends in recent years, but the precipitation has been more spatially heterogeneous across regions (Chinchorkar, *et al.*, 2015; Bal *et al*., 2016; Buri *et al*., 2022). The precipitation trend analysis using the historic events of Kolli Hills, India, showed no significant trend in the annual precipitation of the study area but, at the same time a significant decreasing trend in the southwest monsoon, which was compensated by an increasing trend in the seasonal precipitation of the northeast monsoon (Remya, *et al*., 2015). Annual and seasonal rainfall variability was highest in Western part of India's sub-divisions, while the lowest was found in Eastern and North India. Mann-Kendall test on overall annual and seasonal rainfall reported that the sub-divisions of North-East, South and Eastern India showed a significant negative trend, while the other sub-divisions recorded a positive trend (Praveenkumar and Jothiprakash, 2020). Long-term analysis using the historic dataset in Ananthapuram, Andhra Pradesh, India, revealed that an increase in the summer rainfall trends and decreasing monsoon rainfall trends would impact the agriculture sector in the region (Patakamuri, *et al.*, 2020). Mehta and Yadav (2021) analysed the rainfall variability and drought for 102 years from 1901 and 2002 over Barmer District of Rajasthan, India. Trend analysis of seasonal and extreme annual monthly rainfall depicted that increasing trend was observed in pre, post, southwest monsoon and annual rainfall and a decreasing trend in winter rainfall.

Assessing historic and future trends in meteorological parameters at different spatial and temporal scales plays a crucial role in understanding climate change and its implications for food security, natural resource management, and sustainable development (Praveen and Ramachandran, 2015; Patel, *et al.,* 2021). Therefore, continuous rainfall studies need to be emphasized for long-term water resource planning and management. Most of the studies related to spatio-temporal analysis and trend analysis of climate variables were carried out at district or state or country level (Patakamuri, *et al.*, 2020; Abhilash, *et al.*, 2022; Subrat *et al.,* 2023). Few studies of climate variables variability and trend analysis have been conducted at the basin scale using the historic data set (Praveenkumar and Jothiprakash, 2020; Supriya and Krishnaveni, 2018). Long–term basin-scale studies help address current and future climate change challenges.

General Circulation Models (GCMs) are complex mathematical models that simulate physical processes occurring in the atmosphere, ocean, and land surface. These GCMs are utilised to predict the effects of climate change on hydrologic systems. Evaluating the reliability of individual GCM in simulating the historical climatic parameters to identify the ideal GCM models using various performance indicators. In order to evaluate the suitable model 24 CMIP5-GCMs for the Upper Narmada river basin in India, Pandey *et al*. (2019) employed the Skill Score, Root Mean Square Error, and Total Index (TI) indicators. MIROC5, CNRM-CM5, and MPI- ESM- LR were the best GCMs for the basin. Deepthi *et al*. (2020) examined the suitable GCMs for predicting future precipitation in the Upper Godavari sub-basin, India. Method for rating the GCM was based on performance indicators using Technique for Order Preference to the Similarity to Ideal Solution. The CNRM-CM5-2, CNRM-CM5, and MPI-ESM-P GCMs were suitable for predicting precipitation in the sub-basin using a group decision-making technique. Shaikh *et al*. (2022) studied the climatic projections of Western India using global and regional climate model for the climate variables precipitation, temperature minimum and maximum in Hathmati River watershed. CMIP5 models, namely CCSM4 and CESM1- CAM5 is bias corrected for the observed data and CCSM4 is selected further for climate projection under RCP 4.5 scenario. All the climate variables such as precipitation, minimum and maximum temperature showed a significant increase in the mean value when compared to the baseline (1980 –2019).

From the literature, it is observed that there is a wide range of single and multiple Performance Criteria Analysis (PCA) and decision making methods chosen for ranking of GCMs. In the river basins of India, future

climate change impact studies need to be considered on a case to case basis. Previous research found that the competence of the climate model's performance was region-specific, with significant variability in climatic pattern simulation (Raju and Kumar, 2020; Hassen *et al.*, 2020). Hence, choosing the most appropriate GCMs is suggested for the climate change impact studies of basins. The main objective of this paper is to examine variability and trends of precipitation for the historical period (1901-2020) and the future period (2025 to 2099) using the best-fitted high resolution climate model for the study area.

2. Study area

The Palar River is one of the major sources of water that replenish the groundwater in Vellore, Kanchipuram, and Thiruvanamalai from West to East. Palar is a seasonal river that contributes to the high urbanization area. The two-phase shift occurred before the active river path due to the intensified northeast monsoon, mild neotectonics activity, and rapid upstream avulsion (Resmi, *et al.*, 2017). The availability of surface water in the Palar basin has decreased over the years (Venkatesan, *et al.*, 2019). Groundwater has become the main source for irrigation and drinking water sectors (Krishnan and Saravanan, 2022). The basin covers predominantly Archaean crystalline formations like gneisses and charnockites, and the remaining are alluvium deposits. The Eastern Ghats ranges of hills, the plateau region and the coastal plains are the three main topographical divisions of this basin. The pediment pediplain erosional landform with a very gently sloping (towards the bay of bengal) inclined bedrock surface is predominant. Along the river course, the active flood plain ranges up to 5 km. The occurrence of groundwater is a rare source in the hill and valley region of the upper part of the basin.

The catchment area of the basin is 10228.35 Km^2 and lies between the geographic coordinates of Latitude 12°39' N and 12°54' N & Longitude 78°32' E and 79°56' E. The basin receives an average annual rainfall of 1065.14 mm. The average minimum and maximum temperatures are around 23.54 °C and 33.29 °C. The basin covers urban, peri-urban and rural areas. Rapid migration of the people into the peri-urban area leads to water scarcity and pollution. Extreme climatological events that trigger floods and droughts. It has subsequent impacts on land, and biodiversity. Basin stakeholders rely on the replenishment of the hydrological system by means of monsoon rainfall. The basin is at risk to drought and flood due to the radial increase of the built-up areas, population growth, and over - exploitation of groundwater (Senthil kumar and Elango, 2004; Kanagaraj *et al.*, 2018; Saravanan *et al.*, 2020). An attempt is made in this study by reviewing the previous studies and identifying the research gap. The trend pattern of the historic and future climate variables is mandatory due to scarce availability of the water resources in the basin to empower the understanding of the realistic problem.

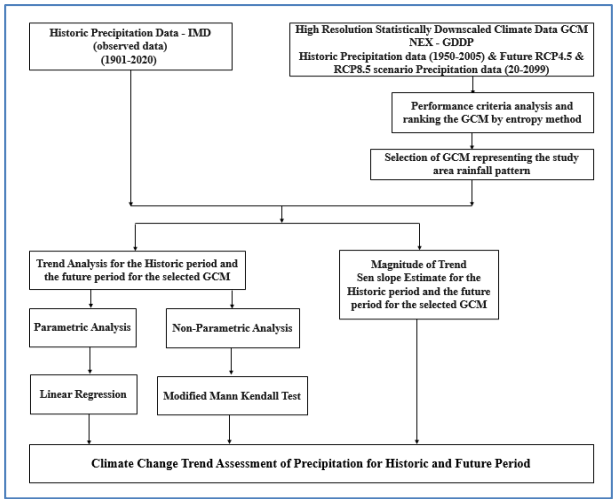

Fig. 1. Flowchart of methodology adopted in this study

3. Methodology

The detailed methodology implemented in this study is discussed in Fig. 1. Indian Meteorological Data (IMD) high resolution, gridded rainfall data at 0.25° × 0.25° resolution for the period of 1901–2020 is used in the study for historic rainfall analysis (Pai, *et al.*, 2014). IMD daily grid rainfall was developed from more than 3,000 rain gauge network stations across India and the grid points are exported for the study area. The grid points locations and their elevations in the study area are shown in table 1.

A statistically downscaled bias-corrected subset of climate scenarios derived from the GCM NASA Earth Exchange-Global Daily Downscaled Projections (NEX-GDDP) dataset over India for two emission scenarios Representative Concentration Pathways (RCPs) 4.5 (moderate emission) and 8.5 (high emission) is used for the future precipitation analysis (Thrasher, *et al.*, 2012). Out of 21 bias-corrected high-resolution (0.25° × 0.25°) datasets, the best-fitted GCM is employed in the study to assess the future climate change impacts on systems from 2025 - 2099. The position of the grid points and the elevation of the IMD data and 21 GCM located in the study area are extracted and presented in Table 1 & Fig. 2.

3.1. *Selection Of GCM*

The performance criteria of each GCM are analysed using Taylor's diagram & the six - efficiency criteria. The Taylor diagram is particularly useful for comparing model strengths & estimating a model's overall

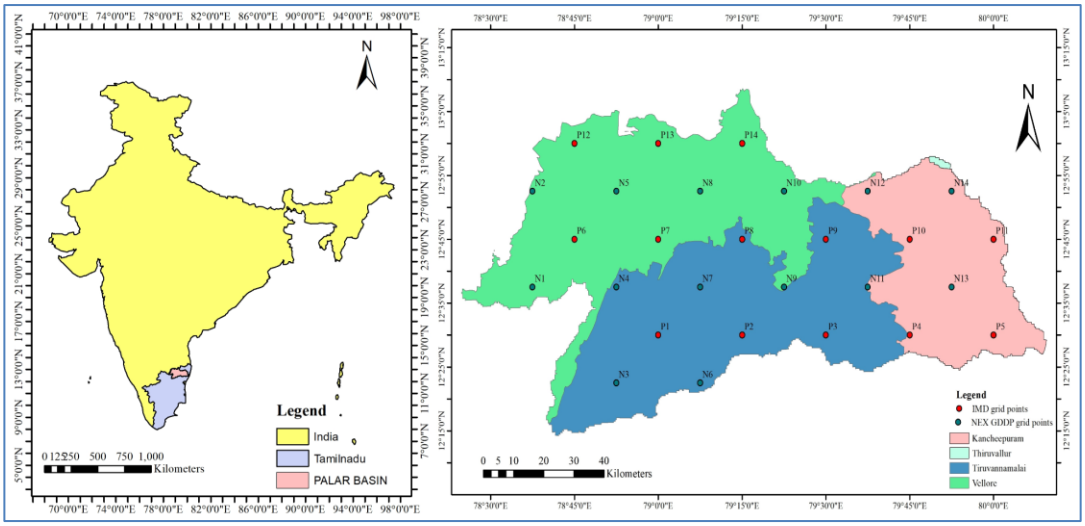

Fig. 2. Location of study area and grid point

TABLE 1

Description of a grid point in the study area considered for analysis of historic IMD

Grid Point	IMD grid point locations – Historic period				NEX-GDDP grid point locations – Future period			
	Latitude	Longitude	Elevation (m)	Annual Average Rainfall (mm)	Latitude	Longitude	Elevation (m)	Annual Average Rainfall (mm)
P1	79	12.5	209	1054.89	N1	12.625	78.625	1054.89
P2	79.25	12.5	164	1082.50	N2	12.875	78.625	1082.50
P3	79.5	12.5	104	1115.05	N3	12.375	78.875	1115.05
P4	79.75	12.5	46	1163.84	N4	12.625	78.875	1163.84
P5	80	12.5	18	1256.63	N5	12.875	78.875	1256.63
P6	78.75	12.75	476	917.89	N6	12.375	79.125	917.89
P7	79	12.75	651	1025.9	N7	12.625	79.125	1025.9
P8	79.25	12.75	159	1047.3	N8	12.875	79.125	1047.3
P9	79.5	12.75	116	1136.43	N9	12.625	79.375	1136.43
P10	79.75	12.75	63	1186.02	N10	12.875	79.375	1186.02
P11	80	12.75	45	1276.37	N11	12.625	79.625	1276.37
P12	78.75	13	410	937.78	N12	12.875	79.625	937.78
P13	79	13	292	997.11	N13	12.625	79.875	997.11
P14	79.25	13	201	951.99	N14	12.875	79.875	951.99

performance (Nash and Sutcliffe, 1970; Raju and Kumar, 2020; Hassen *et al*., 2020). The 'reference field' is one that often represents an observed state, and another is the 'test field' (typically a model-simulated field). The test field should be similar to the reference field to achieve the goal. The indices of the efficiency criteria Root Mean Square Error ($RMSE$), Nash Sutcliffe model Efficiency coefficient (NSE), Pearson coefficient (r), Mean Bias Error (MBE), Mean Absolute Error (MAE), and index of agreement (d) are also calculated. The observed data are denoted as $X_{observed}$ the model data as Y_{model} for i years (i = 1,2,3…, n), $\overline{X}$ is the mean of the observed data, $\overline{Y}$ is the mean of the model data.

The $RMSE$ of average error is calculated by root mean square error between the actual and the predicted model values. $RMSE$ is always non-negative, and the value of '0' indicates a perfect fit to the data.

$$RMSE = \sqrt{\frac{\sum_{i=1}^{n} (X_{observed,i} - Y_{model,i})^2}{n}}$$

NSE indicates the accuracy of the model and plots of the observed versus simulated data to fit in 1:1 line. The value of NSE closer to '1' indicates the perfect agreement with the observed data and '0' indicates that the model has the exact prediction as the observed mean (Taylor, 2001). NSE is between $-\infty$ and +1 for a perfect correlation between the observed and the model prediction data.

$$NSE = 1 - \frac{\sum_{i=1}^{n}(X_{observed,i} - Y_{model,i})^2}{\sum_{i=1}^{n}(X_{observed,i} - \overline{X})^2}$$

The 'r' is a measure of the strength of the linear relationship between the observed and predicted values. The value of r = "1" indicates perfect association with the model prediction and "0" indicates no association.

$$r = \left[\frac{\sum_{i=1}^{n}(X_{observed,i} - \overline{X})(Y_{model,i} - \overline{Y})}{\sqrt{\sum_{i=1}^{n}(X_{observed,i} - \overline{X})^2}\sqrt{\sum_{i=1}^{n}(Y_{model,i} - \overline{Y})^2}}\right]$$

MBE captures the deviation in the prediction. A positive value indicates that the models overestimate the observed data and vice versa.

$$MBE = \frac{1}{n}\sum_{i=1}^{n}\left(X_{observed,i} - Y_{model,i}\right)$$

MBE is calculated between the observed and the predicted value; it can be positive or negative, so the absolute error must be calculated. MAE is the average of the absolute differences between the predicted and actual observation across the test samples. The lower value of MBE indicates the best performance of the model.

$$MAE = \frac{1}{n}\sum_{i=1}^{n}\left|X_{observed,i} - Y_{model,i}\right|$$

The index of agreement (d) is not a correlation measure. It is a measure of the extent to which a model's prediction is error-free. The 'd' is calculated to vary between 0 and 1. The computed value of 1.0 indicates perfect agreement between the observed and predicted values, and 0.0 indicates complete discrepancies.

$$d = 1 - \frac{\sum_{i=1}^{n}(X_{observed,i} - Y_{model,i})^2}{\sum_{i=1}^{n}(|Y_{model,i} - \overline{X}| + |X_{model,i} - \overline{X}|)^2}$$

The NEX-GDDP GCM for 21 CMIP5 climate models ranking is done using the entropy method. The analysis using the entropy method is based on the available data and its relationship with the performance indicators (Banda, *et al.*, 2021). The entropy method measures the weight of each performance indicator separately and finds the difference between the records in the payoff matrix. Weights calculated by the entropy method are assigned to the performance indicators for ranking the models based on multi-criteria decision methods. The entropy of the matrix (E_k) is given by the following equation:

$$E_k = \frac{-1}{ln\,(n)}\sum_{i=1}^{n} p_{ik} ln\,(p_{ik})$$

where p_{ik} is the payoff matrix, E_k is the entropy value for indicator 'k', and 'n' is the number of GCM. The degree of diversification (D_k) represents the value provided by the result of the performance indicator 'k' and is expressed as follows:

$$D_k = 1 - E_k$$

Normalized weights(w_k) of the performance indicators obtained by the entropy method are given below:

$$w_k = \frac{D_k}{\sum_{k=1}^{n} D_k}$$

The NEX- GDDP GCM data set of 21 GCM for the historic and future scenarios is exported to the study region which covers all grid points. The historic climate variable dataset of the climate models from 1950 to 2005, are compared with the observed climate variables for monthly and annual time scale. The efficiency criteria of each model are estimated using the observed data. The Taylor's diagram is also plotted to identify the best fit model. The Multi criteria decision making entropy ranking method is used to rank the model and to identify the best fit model for the study basin for prediction of future precipitation scenarios.

3.2. *Trend Analysis Method*

Parametric and non-parametric approaches identify significant trends in time series analysis. The time-series data should be homogenous and independent. Non-parametric trend tests primarily assume that the data are independent and do not assume statistical distribution. In this study, the trend pattern of precipitation is determined using two non-parametric approaches, Mann-Kendall and Sen's slope estimator.

3.3. *Modified Mann-Kendal Test*

Mann–Kendall (MK) trend test is a non-parametric method most commonly used to investigate trends in hydro-meteorological, climate and environmental data (Mann, 1945; Chinchorkar, *et al.*, 2015). Although the classic MK test is used to identify trends in time series, it may not be appropriate when the serial correlation in the data is too high. In this study, a modified MK test proposed by Yue and Wang (2004) was implemented, in which the influence of serial correlation on the MK test

was investigated by Monte-Carlo simulation. The serially correlated data are first detrended and the effective sample size is calculated using significant serial correlation coefficients.

3.4. *Sen slope estimator*

Sen (1968) developed the non-parametric technique for estimating the trend slope. For the given time series x with n observations in the sample of N data pairs:

$$S = \frac{x_k - x_j}{k - j}, k \neq j$$

where x_j and x_k are the values at times j and k (j>k), respectively.

According to the Sen's method, the overall estimator of the slope is the median of these N values of S. The overall Sen slope estimator S^* is as follows:

$$S^* = S_{\frac{(N+1)}{2}}, N \text{ is odd}; \frac{S_{\frac{N}{2}} + S_{\frac{(N+2)}{2}}}{2}, N \text{ is even}$$

4. Results and discussion

4.1. *Selection of GCM*

The results of the selection of GCM are determined using the Taylor's plot and the PCA. The performance of the historic data (1950-2005) of 21 GCM climate models is evaluated using the Taylor diagram (Fig. 3). The precipitation correlation of all 21 GCM's ranges from 0.4 to 0.6, and the RMS varies from 85 mm/day to 120 mm/day. The historic precipitation of GCM 'MIROC ESM' and 'MIROC ESM CHEM' has a good correlation of 0.6 and RMS difference of 85 mm/day.

The PCA is performed using 6 efficiency criteria for the annual and monthly dataset for the 21 GCM's. The objective weights are assigned to the 6 criteria using the entropy multi criteria decision making method, and the model is ranked. The objective weights assigned for the performance criteria are: NSE - 0.272, MBE – 0.153, d – 0.074, RMSE – 0.077, MAE – 0.034, r – 0.390. In the monthly and annual analysis, MIROC ESM was ranked '1' as shown in Fig. 4. Although the index of agreement of MIROC ESM CHEM, monthly precipitation analysis is greater than that of MIROC ESM, the other analysis has placed the efficiency criteria that has put forward MIROC ESM to rank '1'. In the annual analysis of precipitation GCM data, MIROC ESM performed as a good model in all criteria. The analysis of the Taylor's diagram and the performance of the efficiency criteria exposed that MIROC ESM was a good performance model. Hassen *et al*. (2020) examined the selection of CMIP5 GCM ensemble of the four top-ranked GCMs, namely ACCESS1.3, MIROC-ESM, MIROC-ESM-CHM, and NorESM1-M for the projection of spatio-temporal changes of precipitation and temperature in the Niger Delta, Nigeria. MIROC5, CNRM-CM5 and MPI-ESM-LR were found to be the best performing climate models out of 24 CMIP5 GCM in Upper Narmada Basin (Pandey *et al*., 2019). The selected representative GCM MIROC ESM was the one of the top representative models that represent the Indian climatic conditions reported by researchers and could be used to simulate the study area in the future climate change impact studies.

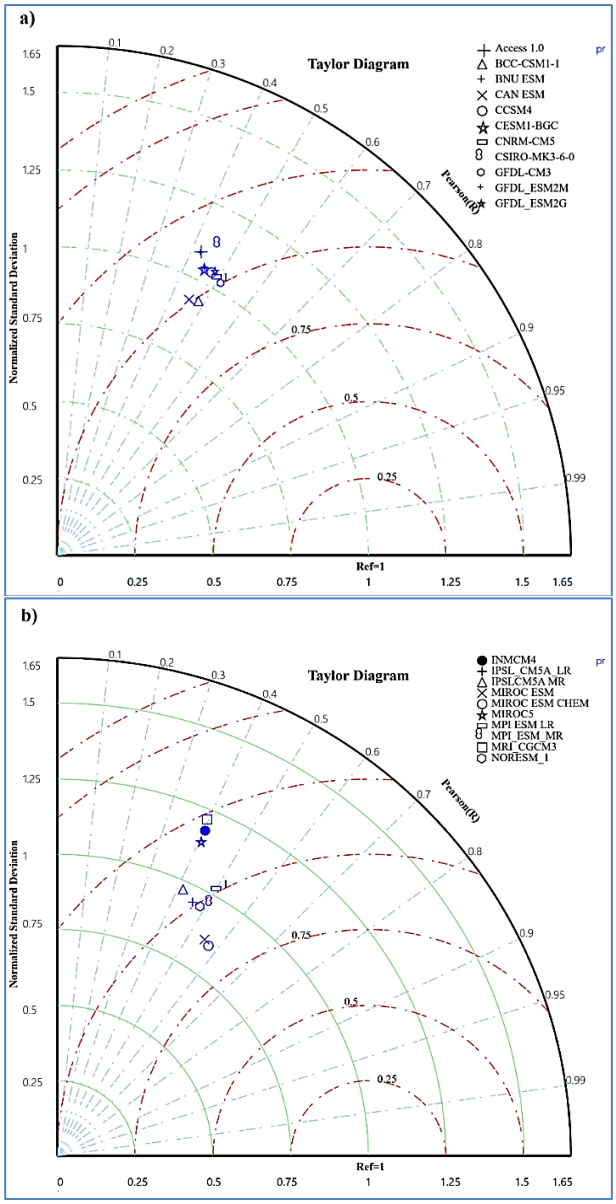

Figs. 3(a&b). Taylor diagram of the GCMs projections a) ACCESS 1.0 to GFDL ESM2G b) INMCM4 to NORESM_1

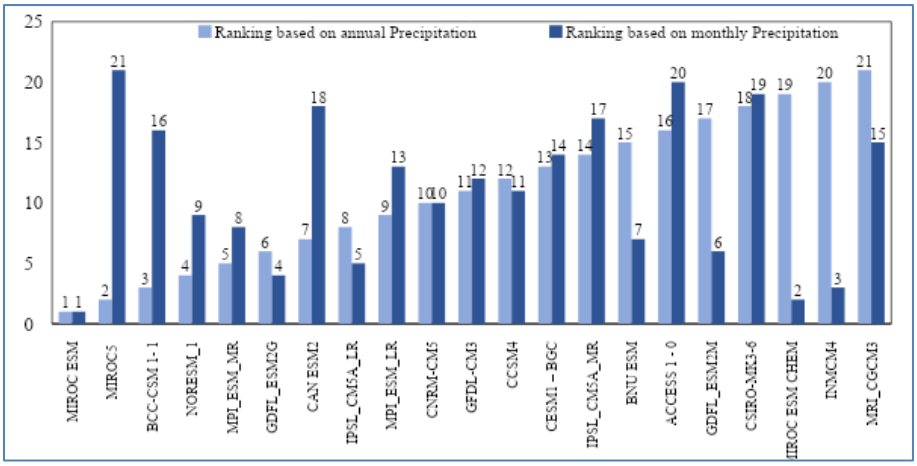

Fig. 4. Ranking of NEX-GDDP GCM for annual and monthly precipitation

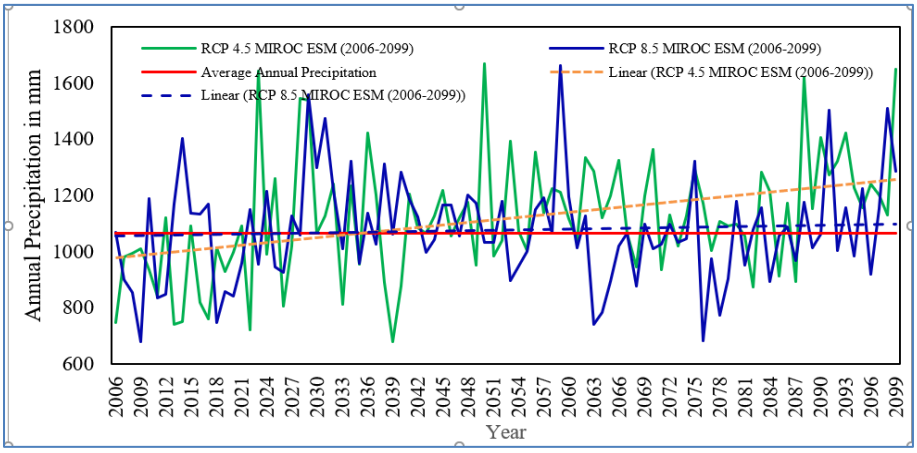

Fig. 5. Annual average future rainfall projections from MIROC ESM GCM

TABLE 2

MK test analysis and magnitude for the historical precipitation

Station No	Annual	JF	MAM	JJAS	OND	Sen slope mm/year
P1	No Trend	↓Trend Detected	↓Trend Detected	No Trend	No Trend	0.036
P2	No Trend	↓Trend Detected	No Trend	No Trend	No Trend	-0.017
P3	No Trend	↓Trend Detected	No Trend	No Trend	No Trend	-0.599
P4	No Trend	↓Trend Detected	No Trend	↓Trend Detected	No Trend	-1.798
P5	No Trend	↓Trend Detected	No Trend	No Trend	No Trend	-0.426
P6	↑Trend Detected	↓Trend Detected	No Trend	↑Trend Detected	No Trend	0.880
P7	No Trend	↓Trend Detected	No Trend	No Trend	No Trend	-0.134
P8	No Trend	↓Trend Detected	No Trend	No Trend	No Trend	0.517
P9	No Trend	↓Trend Detected	No Trend	No Trend	No Trend	0.768
P10	No Trend	↓Trend Detected	No Trend	No Trend	No Trend	-0.734
P11	No Trend	↓Trend Detected	No Trend	No Trend	No Trend	-0.407
P12	No Trend	↓Trend Detected	↓Trend Detected	No Trend	↑Trend Detected	0.121
P13	No Trend	↓Trend Detected	No Trend	No Trend	No Trend	0.042
P14	No Trend	↓Trend Detected	No Trend	↓Trend Detected	No Trend	-0.327

TABLE 3

Change in precipitation of the study area with reference annual average of the base period (2001-2020)

Period	RCP 4.5	RCP 8.5
Near Future (2025-2050)	↑10%	↑11%
Far Future (2051-2099)	↑14%	↑3%

TABLE 4

Sen slope estimator test for the future GCM precipitation

Grid point	RCP 4.5					RCP 8.5				
	Annual (mm/year)	JF	MAM	JJAS	OND	Annual (mm/year)	JF	MAM	JJAS	OND
		(mm/season)					(mm/season)			
N1	0.7436	0.000	0.134	1.680	0.744	0.153	0.000	0.122	0.458	-0.455
N2	0.8206	0.000	0.175	1.760	0.821	0.333	0.000	0.150	0.488	-0.355
N3	0.9404	0.003	0.199	1.555	0.940	-0.140	0.004	0.081	0.304	-0.494
N4	0.9656	0.000	0.159	1.575	0.966	0.109	0.002	0.105	0.516	-0.450
N5	1.0168	0.000	0.174	1.668	1.017	0.346	0.001	0.132	0.517	-0.391
N6	1.0558	-0.011	0.242	1.754	1.056	0.132	0.000	0.036	0.653	-0.481
N7	1.0435	-0.008	0.225	1.861	1.044	0.354	0.000	0.045	0.901	-0.443
N8	1.1185	-0.005	0.223	1.835	1.119	0.316	0.000	0.055	0.920	-0.331
N9	1.2652	-0.013	0.219	1.727	1.265	0.472	0.002	0.039	0.871	-0.451
N10	1.3018	-0.011	0.211	1.739	1.302	0.370	0.001	0.051	0.877	-0.396
N11	1.4497	-0.013	0.177	1.568	1.450	0.535	0.005	0.038	0.898	-0.392
N12	1.5049	-0.015	0.182	1.601	1.505	0.369	0.002	0.045	0.838	-0.376
N13	1.5681	-0.017	0.168	1.462	1.568	0.632	0.008	0.029	0.834	-0.361
N14	1.6811	-0.015	0.181	1.469	1.681	0.480	0.005	0.026	0.823	-0.353

4.2. *Trend Analysis*

The MK statistical test has been widely used to quantify the significance of trends in hydro-meteorological time series.

4.2.1. *Trend and Magnitude Analysis of historic period*

The MK test trend analysis and magnitude of historic precipitation from 1901 to 2020 for annual and seasonal is presented in Table 2. The trend analysis showed increasing and decreasing trends in annual precipitation and seasonal series. At grid point P6 an increasing annual rainfall trend is observed of 95% confidence interval (0.88 mm/year). Rainfall in the southwest monsoon months is 1.009 mm/year at station P6. Other grid points in the historic annual precipitation series show no trend pattern over 120 years (1901-2020). Grid-point location P4 showed an irregular decrease in precipitation (1.798 mm /year) than the other grid points. Grid points P2, P3 of Tiruvannamalai district; P4, P5, P10, P11 of Kanchipuram district; and P7, P14 of Vellore district show decreasing annual precipitation. Grid points P1, P8, P9 of Tiruvannamalai district; P6, P12, and P13 of Vellore district show increasing annual precipitation. The precipitation variation of the study area over 120 years decreased by 0.148 mm/year. The JJAS months showed an increasing trend pattern of 0.048 mm/year from 1901 to 2020. In other seasons JF, MAM, and OND showed a decreasing magnitude of 0.127 mm/ season, 0.063 mm/season, and 0.099 mm/season. In the historical period, the monsoonal forward shift and shortening of the monsoon season happened due to climate change. However, the same trend pattern was observed in the Kanchipuram and Vellore district from the previous studies. Dhanya *et al*. (2015) studied the climate variability in Kanchipuram district for the period of 1970-2000 generally showed a decreasing trend pattern in non-parametric tests. Rainfall distribution in the southwest

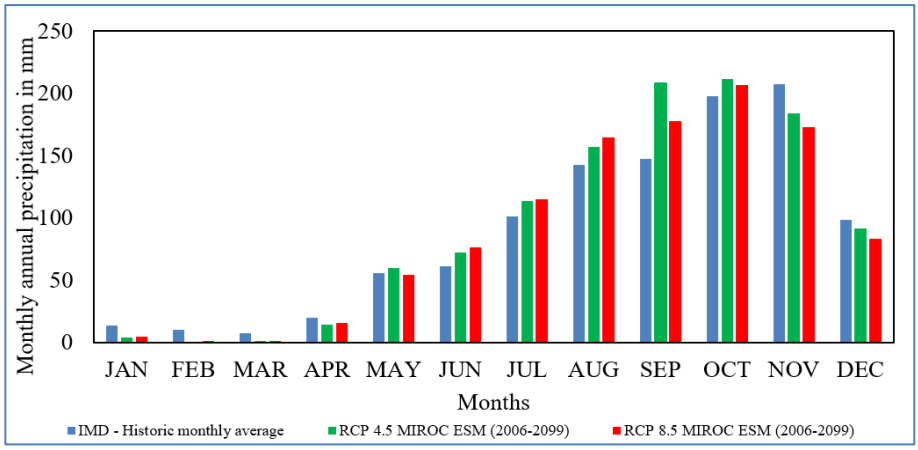

Fig. 6. Future Monthly annual average rainfall projections from MIROC ESM GCM

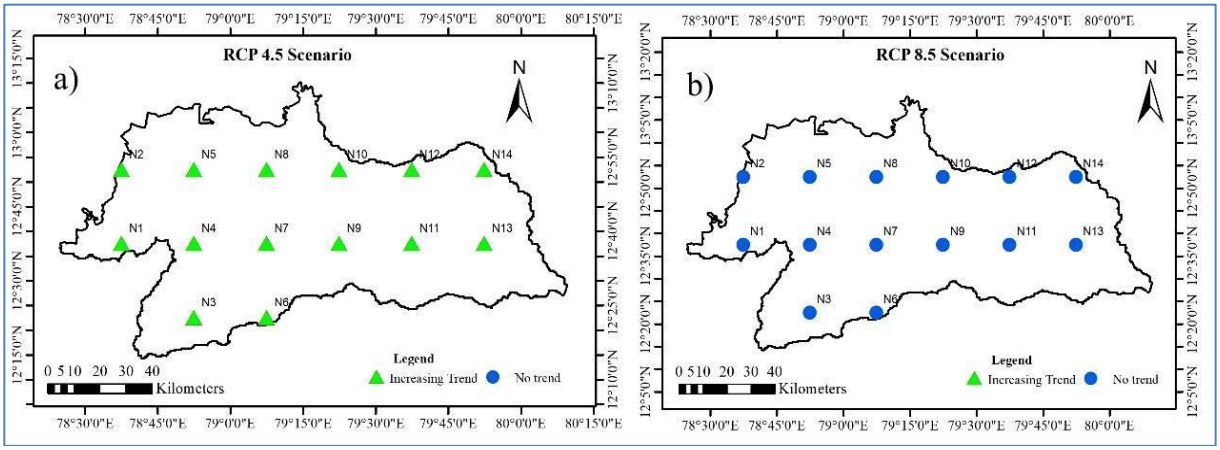

Figs. 7(a & b). MK Trend of future annual rainfall projections a) RCP 4.5 b) RCP 8.5

monsoon season has decreased compared to the northeast monsoon season. The precipitation data for the period of 10 years from 2008 to 2017 for all the 5 rain gauge stations in Vellore district was analysed by Venkatesan *et al*. (2021). The study concluded that moderate annual precipitation was received when compared with the average annual precipitation of Tamil Nadu (920 mm). Pavithrapriya *et al*. (2022) observed that rainfall showed an insignificant decreasing trend in Adirampattinam and Nagapattinam meteorological stations and an increasing trend in the IMD grid points in Thanjavur Delta region of Tamil Nadu for the period of 1970 to 2014. Subrat *et al*., (2023) demonstrated a general decline in yearly monsoon precipitation across most regions in the states Karnataka, Gujarat, Rajasthan, and Maharashtra. Amit et al. (2023) observed the maximum average annual rainfall reduced from 1,769 to 1,401 mm after 1998 affecting water availability in Madhya Pradesh, India. The study highlighted a significant shift in Madhya Pradesh's seasonal rainfall distribution after 1998.

4.2.2. *Trend and Magnitude Analysis of future period*

The linear trend of the annual average precipitation of the study area for the future period from 2006 to 2099 is shown in Fig. 5 for moderate and high emission scenarios. The moderate emissions scenario shows an increasing trend, after 2040 the rainfall will be above the historic annual average. More than 1600 mm of precipitation can be expected in the periods 2023, 2050, 2088, and 2099, which is 50% more than the annual average under scenario RCP 4.5. The years 2029, 2059, 2091, and 2098 may be expected to have more than 1400 mm of rainfall, 30% more than the annual average of the scenario RCP 8.5.

The monthly average of historical and future precipitation is portrayed in Fig. 6. Rainfall is observed to increase in the months of August, September, and

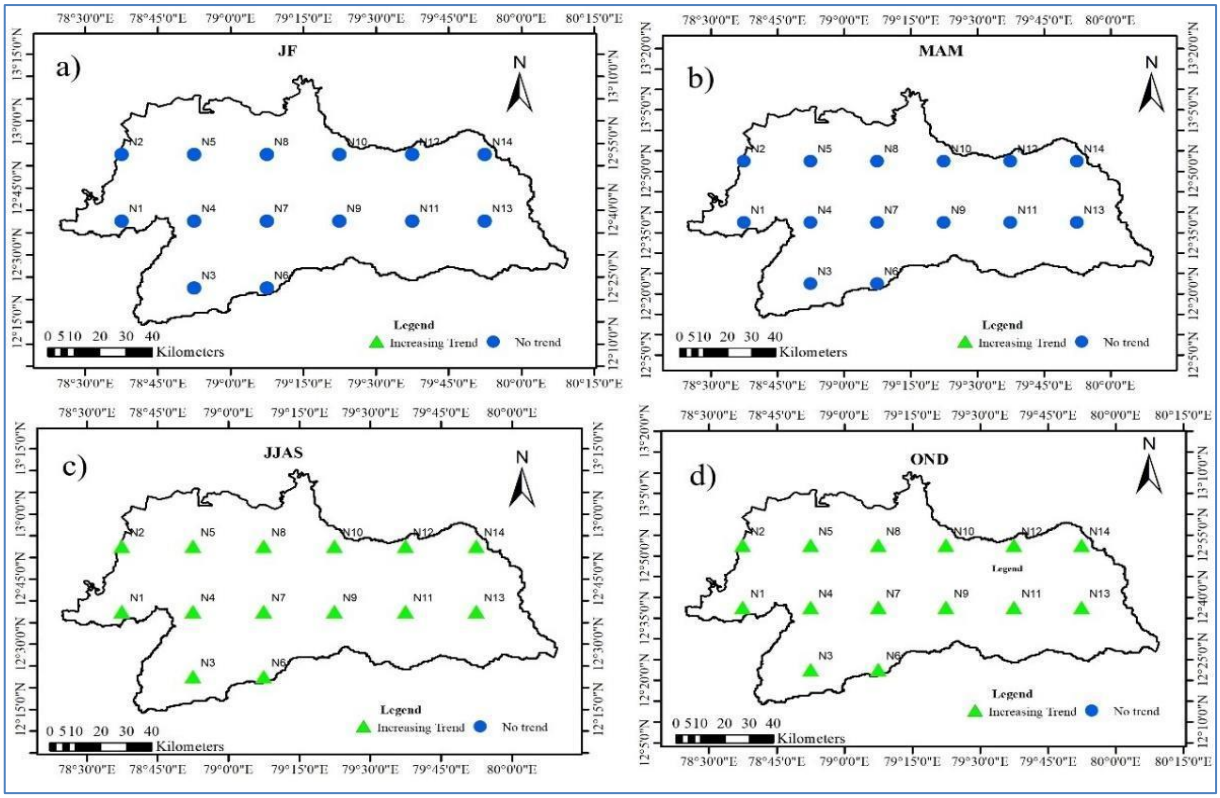

Figs. 8(a-d). MK Trend of future seasonal rainfall projections of RCP 4.5 a) JF b) MAM c) JJAS d) OND

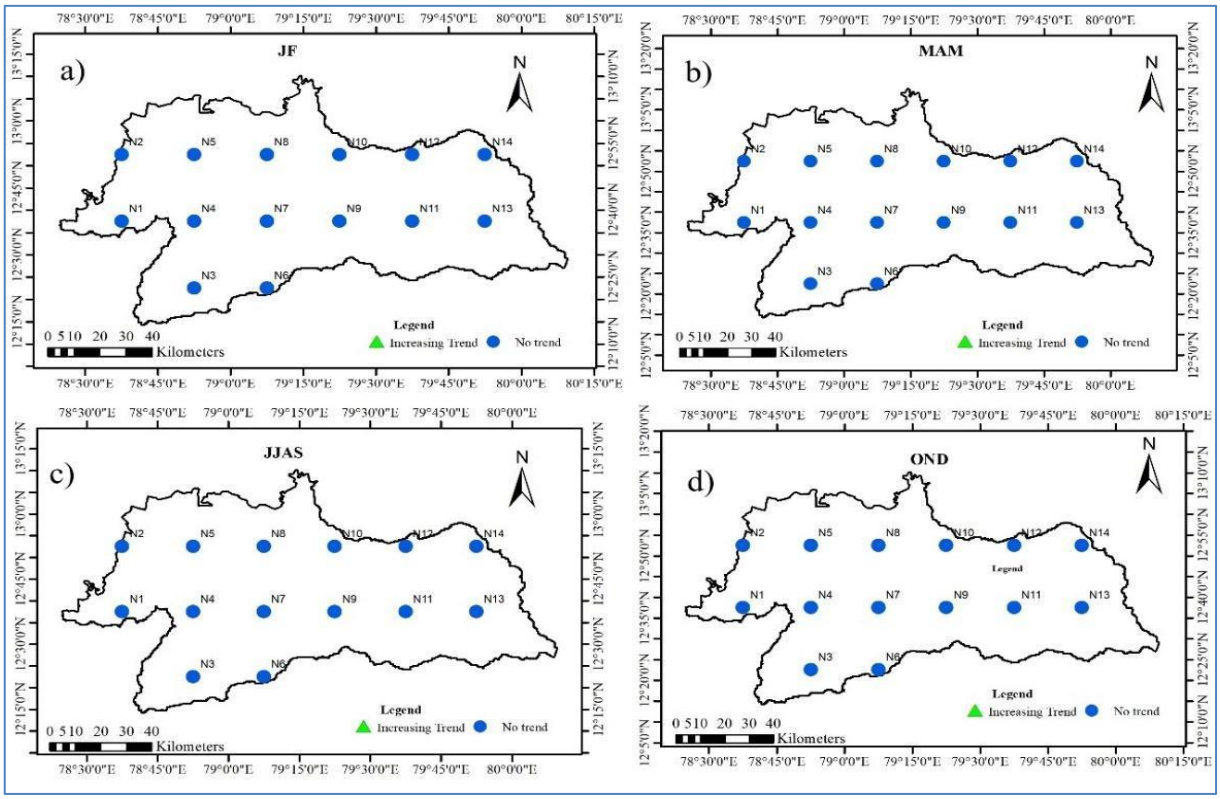

Figs. 9(a-d). MK Trend of future seasonal rainfall projections of RCP 8.5 a) JF b) MAM c) JJAS d) OND

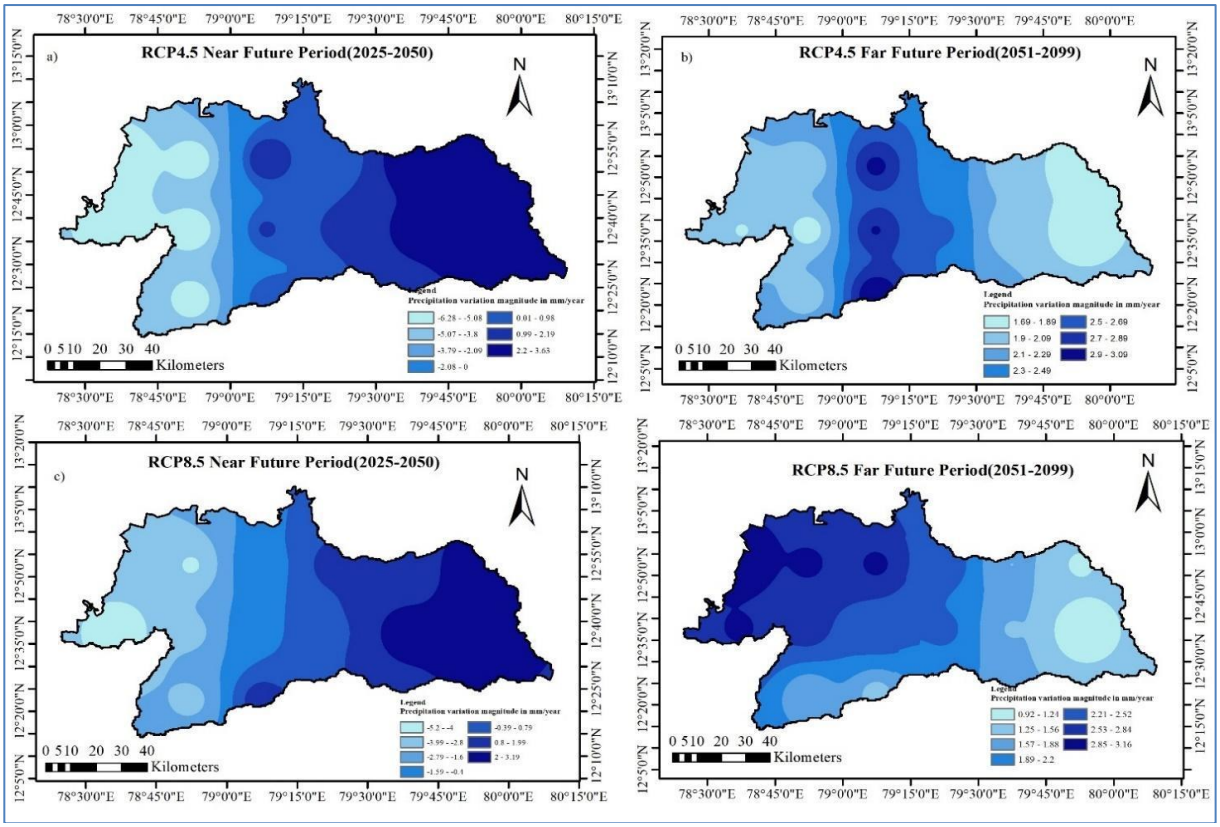

Figs. 10(a-d). Spatial variation of annual precipitation in near future period and far future period for RCP 4.5 and RCP 8.5 Scenario

October when compared with the baseline period (1901-2020) for both scenarios. It is also noted that there is an increase in the amount of precipitation in southwest monsoon (JJAS) compared with the northeast monsoon (OND). There is a slow shift in the paradigm of monsoonal forward shift and monsoon period reduction has happened due to climate change. Geetha and Raj (2015) also synchronised with the findings observed with the historical precipitation major shift that withdrawal of northeast monsoon from north coastal Tamilnadu occurs about 2 weeks prior to the withdrawal from the central and southern parts of coastal areas in Tamilnadu.

Trend analysis is performed for the future MIROC ESM GCM precipitation dataset from 2025 to 2099 in annual and seasonal time scales shown in Figs. 7, 8 and 9. The change in precipitation variation for the near and far future period with respect to actual rainfall observed in the basin from 2000 to 2020 is presented in Table 3. The average annual precipitation of the near future period for the moderate and high emission scenarios are 1129.02 mm and 1148.84 mm. For the moderate and high emission scenarios, the average annual precipitation for the far future period is 1176.14 mm and 1065.15 mm, respectively. The moderate emissions scenario shows an increasing trend pattern in the annual and monsoon months (JJAS and OND). The high emission scenarios do not show a significant trend pattern in the annual and seasonal analysis. The Sen slope estimation analysis shown in Table 4 describes the magnitude of the trend variation for the future period. The southwest monsoon month (JJAS) will receive an increase in precipitation of 1.462 to 1.861 mm/season above normal rainfall in the moderate emission scenario and 0.304 to 0.920 mm/season of rainfall in the high emission scenario. The northeast monsoon month (OND) will receive an increase of 0.744 to 1.681 mm/season above normal rainfall in moderate emission. However, the high emission scenario in OCD shows a decreasing magnitude of 0.331 to 0.494 mm/season. The summer rainfall (MAM) has increased by 0.2 mm/season but does not follow any trend pattern in moderate emission. The JF seasonal does not show any significant trend in the future period.

The spatial variation in annual precipitation in the near future (2025-2050) and far future period (2051-2099) is shown in figure 10. In both scenarios of the near future, the magnitude of precipitation variation resembles the same. The upper reach of the basin receives less precipitation in the moderate emission scenario than the

average annual rainfall of about ~ 5 mm/year where groundwater was extinct. The moderate emission scenario shows the increased amount of rainfall of about 1.69 – 3.09 mm/year in the far future period of the annual precipitation. The high emission scenario shows the increased amount of rainfall of about 0.92 – 3.16 mm/year in the far future period of the annual precipitation. The middle and lower reach of the basin receives high rainfall during the monsoonal season, where urbanization clustering has increased in recent years. Future summer rainfall magnitude is increased compared to the historical period due to coastal upwelling. The annual rainfall projections of the RCP4.5 scenario in near future and far future period with the range of 680 - 1670 mm/year and 876 - 1649 mm/year. Annual rainfall forecasts for the RCP8.5 scenario in the near and far future range from 926 - 1558 mm/year to 685-1664 mm/year. Dhanya *et al*. (2013) observed the projected climate variability of Kanchipuram district using the A1B scenario using the PRECIS Regional Climate Model. The rainfall projections showed decreasing trends for annual mean rainfall with a range of 700 - 1200 mm for the entire district during the period 2040 - 2070 with reference to the baseline period (1970 - 2000). The western part of the district shows the rainfall distribution of 700 - 900 mm/year and 750 - 950 mm/year for the period 2040 - 2070 and 2070 - 2100.The eastern and the coastal part of the district shows the 950-1200 mm/year and 1000 - 1250 mm/year for the same projection period. Pavithrapriya *et al*. (2022) remarked that an insignificantly decreasing trend of rainfall over the period 2015 - 2050 in Thanjavur Delta region of Tamil Nadu under RCP 4.5 emission scenario of MPI_ESM_LR CMIP5 model. Shaikh *et al.* (2022) showed an increase in precipitation to 1015.54 mm from 936.91 mm in 2050s projections. The average precipitation is increased around 8.45% with respect to the base line period of 1980 to 2019 using RCP4.5 projections of CCSM4 GCM simulations. Pandey (2023) used RegCM4-4CCCma-CanESM2 model in Gujarat, India to simulate the annual rainfall. It was found to increase during the projected period of 2020-2099 at the rate of 11.6 mm/decade under RCP 4.5 and 36.7 mm/decade under RCP 8.5.

5. Conclusions

Precipitation is a meteorological element that is highly variable in space and time. A key strength of the research is that precipitation analyses are performed for the historical and future basin level datasets. The significant findings of the study are that historic temporal variability and magnitude of precipitation change is less compared with future scenarios. Annual precipitation for the 120 years (1901-2020) shows no trend pattern, but the JF months show a decreasing trend pattern over the historical period indicating the forward shift of the monsoonal months. PCA according to Taylor's diagram and efficiency criteria has revealed that MIROC ESM is a good performer model out of 21 NEX-GDDP GCM, that simulates the study basin climatology. MIROC-ESM was used to study the future climate change impact and predict future climate change scenarios in the Palar basin. The first half from 2006 to 2099 receives less annual rainfall than the second half in the moderate emission scenario and vice versa in the high emission scenario. The annual and monsoon months show an increasing trend of 1 mm/year in the entire basin at each grid point in the moderate emission scenario. The precipitation projection of the high emission scenario does not show a trend pattern but an increased variability of 0.5 mm/year at each grid point will be observed. In the first decade of the 21st century, the rainfall in the study area resembles the RCP 4.5 scenario, and the second-decade pattern resembles the RCP 8.5. Average precipitation may increase by 1030.40 + 98.58 mm in the near future period and 1030.40 + 145.68 mm in the far future period in the RCP 4.5 scenario. The condition of high emission scenario would increase the precipitation by 1030.40 + 118.42 mm in the near future period and 1030.40 + 34.7 mm in the far future period with reference to the annual average rainfall received in the study area during 2000-2020.

The basin with the topography of ghats, plateau, and coastal region with increased precipitation and urban sprawl can directly result in significant hazards like rapid runoff, urban flooding, and flood discharge. The extreme flood and drought events of recent years are omens for the future. In a focused view of the future precipitation variability with reference to historic period events the water managers can rejuvenate the basin's water holding capacity. The rainfall-runoff and groundwater recharge rate projection studies in the basin would be future challenges that would help water resource managers to implement the policy. The precipitation analysis studies of a historical and future scenario provide insights into distinguishing vulnerable zones within the Palar basin that would help the stakeholders in preliminary planning and decision-making for integrated water resources management.

Acknowledgement

The authors of this paper would like to acknowledge the IMD and NEX-GDDP. The historical IMD dataset is freely available on the website of India Meteorological Department, Pune, India (https://www.imdpune.gov.in/). The NEX-GDDP GCM dataset for historic, RCP 4.5 and 8.5 scenario is freely available on the website of Centre for Climate Change Research, Indian Institute of Tropical Meteorology, Pune, India (https://cccr.tropmet.res.in/home/nex_gddp_india.jsp).

Authors' contributions

Nandini Krishnan: Analysed and interpreted the data, prepared figures and wrote the original manuscript. (*email-knandini2018@gmail.com*).
Suriya Saravanan: Reviewed and edited the manuscript.
All authors read and approved the final manuscript.

Disclaimer: The contents and views presented in this research article/paper are the views of the authors and do not necessarily reflect the views of the organizations they belong to.

References

Abhilash, S.C., Surender, S., Rajesh, K. S. M., Alka, R. and Abhishek, D., 2022, "Spatio-temporal trend analysis and future projections of precipitation at regional scale: a case study of Haryana, India", Journal of Water and Climate Change. **139**, 5, 2143–2170.

Amit, K., Siddharth, K., Kuldeep, S.R., Sulochana, S., Tapas, R. and Mohanasundari, T., 2023, "Assessing seasonal variation and trends in rainfall patterns of Madhya Pradesh, Central India", Journal of Water and Climate Change, **14,** 10, 3692-3712. https://doi.org/10.2166/wcc.2023.280.

Bal, P.K., Ramachandran, A., Geetha, R., Bhaskaran, B., Thirumurugan, P., Indumathi, J. and Jayanthi, N., 2016, "Climate change projections for Tamil Nadu, India: deriving high-resolution climate data by a downscaling approach using PRECIS", *Theoretical and Applied Climatology*, **123**, 523–535. https://doi.org/10.1007/s00704-014-1367-9.

Banda, V.D., Dzwairob, R.B., Singh, S.K., and Kanyerere, T., 2021, "Trend analysis of selected hydro-meteorological variables for the Rietspruit sub-basin, South Africa", *Journal of Water and Climate Change*, **12**, 3099–3123. https://doi.org/10.2166/wcc.2021.260.

Buri, E.S., Keesara, V.R., and Loukika, K.N., 2022, "Long-term trend analysis of observed gridded precipitation and temperature data over Munneru River basin, India", Journal of Earth System Science, **131**, 1-18. https://doi.org/10.1007/s12040-022-01864-7.

Chinchorkar, S.S., Sayyad, F.G., Vaidya, V.B., and Pandye, V., 2015, "Trend detection in annual maximum temperature and precipitation using the Mann Kendall test – A case study to assess climate change on Anand of central Gujarat", *Mausam*, **66**, 1–6.

Deepthi, B., Sunil, A., Nair, S. and Mirajkar, A., 2020, "Ranking of cmip5-based general circulation models using compromise programming and topsis for precipitation : a case study of upper godavari basin, India", *International Journal of Big Data Mining for Global Warming*, **2**, 2, 1–25.

Dhanya, P., Ramachandran, A., Prasanta, K. B., and Thirumurugan, P., 2013, "Recent and future weather and climate trends of Kancheepuram, Tamil Nadu and their possible impacts on agriculture", *Journal of Agrometeorology*, **15 (**special Issue II), 176-182.

Fowler, A. M. and Hennessy, K. J., 1995, "Potential impacts of global warming on the frequency and magnitude of heavy precipitation", *Natural Hazards*, **11**, 283–303. https://doi.org/10.1007/BF00613411.

Geetha, B., and Raj, Y. E. A., 2015, "A 140 year data archive of dates of onset and withdrawal of northeast monsoon over coastal Tamil Nadu: 1871-2010 (Re-determination for 1901-2000)", *Mausam*, **66**, 1, 7-18.

Hassan, I., Kalin, R.M., White, C.J., and Aladejana, J.A., 2020, "Selection of CMIP5 GCM ensemble for the projection of spatio-temporal changes in precipitation and temperature over the Niger Delta, Nigeria", *Water* (Switzerland), **12**, 2, 1–19.

Jayanthi, S.L.S.V. and Keesara, V.R., 2020, "Observed and simulated climate variability and trends in a semi- arid region", *Spatial Information Research*, **28**, 129–138. https://doi.org/10.1007/s41324-019-00278-w

Jena, P. and Azad, S., 2021, "Observed and projected changes in extreme drought and flood-prone regions over India under CMIP5 RCP8.5 using a new vulnerability index", *Climate Dynamics*, **57**, 2595–2613. https://doi.org/10.1007/s00382-021-05824-7.

Kanagaraj, G., Suganthi, S, Elango, L. and Magesh, N.S., 2018, "Assessment of groundwater potential zones in Vellore district, Tamil Nadu, India using geospatial techniques", *Earth Science Informatics*, **12**, 211–223.

Krishnan, N., and Saravanan, S., 2022, "Assessment of Groundwater Quality and Its Suitability for Drinking and Irrigation Usage in Kanchipuram District of Palar Basin, Tamilnadu, India", *Polish Journal of Environmental Studies*, **31,** 3, 2637–2649. https://doi.org/10.15244/pjoes/144914.

Majra, J.P. and Gur, A., 2009, "Climate change and health: Why should India be concerned", *Indian Journal of Occupational and Environmental Medicine*, **13**, 11–16. https://doi.org/10.4103/0019-5278.50717.

Mann, H.B., 1945, "Non-Parametric Test Against Trend" Econometrica, **13**, 245–259.

Mehta, D., and Yadav, S.M., 2021, "An analysis of rainfall variability and drought over Barmer District of Rajasthan, Northwest India", *Water Supply*. **21,** 5**,** 2505-2517. https://doi.org/10.2166/ws.2021.053.

Nash, J.E. and Sutcliffe, J.V., 1970, "River flow forecasting through conceptual models part I - A discussion of principles", *Journal of Hydrology*, **10**, 282–290.

Pai, D.S., Sridhar, L., Rajeevan, M., Sreejith, O.P., Satbhai, N.S., and Mukhopadhyay, B., 2014, "Development of a new high spatial resolution (0.25° × 0.25°) long period (1901-2010) daily gridded rainfall data set over India and its comparison with existing data sets over the region", *Mausam*, **65**, 1-18.

Panda, A., 2019, "Trend analysis of seasonal rainfall and temperature pattern in Kalahandi, Bolangir and Koraput districts of Odisha, India", **20**, 1–10. https://doi.org/10.1002/asl.932.

Pandey, B.K., Khare, D., Kawasaki, A., and Mishra, P.K., 2019, "Climate change impact assessment on blue and green water by coupling of representative CMIP5 climate models with physical based hydrological model", *Water Resources Management*, **33**, 141–158. https://doi.org/10.1007/s11269-018-2093-3.

Patakamuri, S.K., Muthiah, K., and Sridhar, V., 2020, "Long-Term Homogeneity , Trend , and Change-Point Analysis of Rainfall in the Arid District of Ananthapuramu, Andhra Pradesh State, India", *Water* (Switzerland) **12,** 1, 1–22. https://doi.org/10.3390/w12010211.

Patel, A., Goswami, A., Dharpure, J.K., and Thamban, M., 2021, "Rainfall variability over the Indus, Ganga, and Brahmaputra river basins: A spatio-temporal characterization", *Quaternary International*, **575–576**, 280–294. https://doi.org/10.1016/j.quaint.2020.06.010.

Pavithrapriya, S., Ramachandran, Ahamed, I. S.N., and Palanivelu, K., 2022, "Climate variability trend and extreme indices for the Thanjavur Delta region of Tamil Nadu in South India", Mausam, **73**, 20, 237-250. https://doi.org/10.54302/mausam.v73i2.5475.

Praveen, D., and Ramachandran, A., 2015, "Projected Warming and Occurrence of Meteorological Droughts-Insights from the Coasts of South India", American Journal of Climate Change, **04**, 173–179. https://doi.org/10.4236/ajcc.2015.42013.

Praveenkumar, C., and Jothiprakash, V., 2020, "Spatio-temporal trend and homogeneity analysis of gridded and gauge precipitation in Indravati river basin, India", Journal of Water and Climate Change. **11**, 178–199. https://doi.org/10.2166/wcc.2018.183.

Raju, K.S., and Kumar, D.N., 2020, "Review of approaches for selection and ensembling of GCMs", Journal of Water and Climate Change, **11**, 3, 577–599.

Ramachandran, A., Palanivelu, K., Mudgal, B.V., Jeganathan, A., Guganesh, S., Abinaya, B., and Elangovan, A., 2019, "Climate change impact on fluvial flooding in the Indian sub-basin: A case study on the Adyar sub-basin", PLoS ONE, **14**, 1-24. doi: https://doi.org/10.1371/journal.pone.0216461.

Remya, K., Ramachandran, A., Jayakumar, S., and Kumar, D.S., 2015, "Rainfall trend analysis of Kolli hill, Tamil Nadu, India", *Mausam*, **66**, 151-154. doi : https://doi.org/10.54302/mausam.v66i1.376.

Resmi, M.R., Achyuthan, H., and Jaiswal, M.K., 2017, "Middle to late Holocene paleochannels and migration of the Palar River, Tamil Nadu: Implications of neotectonic activity", *Quaternary International*, **443**, 211–222. https://doi.org/10.1016/j.quaint.2016.05.002.

Saravanan, S., Pitchaikani, S., and Venkatesan, G., 2020, "Assessment and evaluation of groundwater vulnerability index maps of Upper Palar River Basin, Tamilnadu, India", Journal of Earth System Science, **129**, 1, 1–13.

Senthilkumar, M., and Elango, L., 2004, "Three-dimensional mathematical model to simulate groundwater flow in the lower Palar River basin, southern India", *Hydrogeology Journal*, **12**, 2, 197–208.

Shaikh, M.M., Pradeep, L., Prashant, L., and Darshan, M., 2022, "Climatic projections of Western India using global and regional climate models", *Water Practice & Technology*, **17,** 9, 1818-1825. https://doi.org/10.2166/wpt.2022.090.

Subrat, N., Aneesh, M., Sumit, K., Padala, R.S., 2023, "Rainfall and temperature dynamics in four Indian states: A comprehensive spatial and temporal trend analysis", **6,** 247-254. https://doi.org/10.1016/j.hydres.2023.09.001.

Supriya, P., and Krishnaveni, M., 2018, "Change Point Detection and Trend Analysis of Rainfall and Temperature Series over the Vellar River Basin", Polish Journal of Environmental Studies, **27**, 4, 1673-1681. http://doi.org/10.15244/pjoes/77080

Taylor, K.E., 2001, "Summarizing multiple aspects of model performance in a single diagram", *Journal of Geophysical Research*, **106**, 7183–7192.

Thrasher, B., Maurer, E.P., McKellar, C., and Duffy, P.B., 2012, "Technical Note: Bias correcting climate model simulated daily temperature extremes with quantile mapping", Hydrology and Earth System Sciences, **16**, 3309–3314. https://doi.org/10.5194/hess-16-3309-2012.

Venkatesan, G., Pitchaikani, S., and Saravanan, S., 2019, "Assessment of Groundwater Vulnerability Using GIS and DRASTIC for Upper Palar River Basin, Tamil Nadu", *Journal of the Geological Society of India*, **94**, 387–394. https://doi.org/10.1007/s12594-019-1326-2

Venkatesan, G., Subramani, T., Karunanidhi, D., Sathya, U., and Peiyue, L., 2021," Impact of precipitation disparity on groundwater fluctuation in a semi-arid region (Vellore district) of southern India using geospatial techniques", *Environmental Science and Pollution Research*, **28,** 18539-18551.

Yadav, R., Tripathi, S.K., Pranuthi, G., and Dubey, S.K., 2014, "Trend analysis by Mann-Kendall test for precipitation and temperature for thirteen districts of Uttarakhand", *Journal of Agrometeorology*, **16**, 164–171.

Yue, S.; Wang, C.: The Mann-Kendall Test Modified by Effective Sample Size to Detect Trend in Serially Correlated Hydrological Series. Water Resources Management. 18, 201–218, 2004.